Experiments in Fluids 30 (2001) 286–294 © Springer-Verlag 2001

Tracking of coherent thermal structures on a heated wall by means of infrared thermography

G. Hetsroni, T. A. Kowalewski, B. Hu, A. Mosyak

Abstract This paper deals with measurements of convective velocity of large-scale thermal structures, using the thin foil technique and infrared thermography to visualize the thermal pattern on the wall. An image correlation method is proposed to track the displacement of the observed thermal pattern. The idea of the method is similar to that of particle image velocimetry, but the thermal patterns on the heated wall are used, rather than tracing particles. On this basis, the thermal patterns created by the coherent structures of turbulent channel flow are examined. Particular attention is paid to the determination of the optimal parameters of image acquisition, including spatial and temporal separation. An attempt is made to relate momentum and scalar transport analyses by considering the propagation velocity of large-scale temperature structures. The proposed technique appears to be an attractive alternative for non-intrusive analysis of turbulent flow, especially, where opaqueness of channel walls excludes the use of optical methods.

List of symbols

B	gray level bandwidth
H	water depth
k	thermal diffusivity
u, w	velocities in the streamwise and spanwise directions
u^*	shear velocity
U	mean flow velocity
Pr	k/ν, Prandtl number
u_o	average propagation velocity calculated from experiment
Re	UH/ν, Reynolds number
t	time
T	number of frames in a sequence
n	number of qualified vectors
var(u)	variance of calculated velocities
x, y, z	streamwise, normal and spanwise coordinates

Greek symbols

τ	shear stress
ρ	density
ν	kinematic viscosity

Superscripts and subscripts

+	dimensionless variable
w	value at the wall

Received: 18 January 2000/Accepted: 20 May 2000

G. Hetsroni, B. Hu, A. Mosyak
Department of Mechanical Engineering
Technion – IIT, Haifa
32000 Israel

T. A. Kowalewski
Polish Academy of Sciences IPPT PAN
Swietokrzyska 21, 00-049 Warsaw, Poland
e-mail: tkowale@ippt.gov.pl

Correspondence to: T. A. Kowalewski

This research was supported by the Basic Research Foundation administered by the Israel Academy of Sciences and Humanities and by the Ministry of Science, State of Israel. This research was also supported by the Fund for the Promotion of Research at the Technion. A. Mosyak was partially supported by the Center for Absorption in Science, Ministry of Immigrant Absorption (State of Israel). The authors express their gratitude to Dr. G. Ziskind for his help in the experimental part of the work.

1 Introduction

In spite of extensive experimental, theoretical and numerical efforts, turbulence remains one of the last unsolved important subjects of physics. This is not only due to theoretical difficulties in obtaining a closed description of the phenomenon, but also due to experimental difficulties in obtaining and analysing a representative picture of the flow. In addition, for most of the practical applications where turbulence may play a significant role, side wall opaqueness excludes most of the optical tools such as laser Doppler anemometry, laser-induced fluorescence or particle image velocimetry (PIV), not to mention standard flow visualization.

The typical transition to turbulence gives rise to large-scale coherent structures, defined as persistent flow patterns with a relatively long lifetime and large spatial extent. Hence, their identification, classification and analysis have become important elements of turbulence investigations today (Robinson 1991, 1993).

In general, a turbulent flow field causes fluctuations in a scalar field through turbulent convection, whereas the fluctuating scalar field influences the velocity field through mean gradients and density changes. For small temperature differences, however, the turbulent velocity field drives the scalar field, and the influence of the latter on the former is rather weak and can be neglected. Large-scale

near-wall turbulent motions clearly show the well-known wall layer streaky structures. Kim and Moin (1989) presented results pertaining to the transport of a passive scalar in a turbulent flow. It appears that the scalar fields are highly correlated with the streamwise velocity in the wall region.

One of the possible methods of visualizing the presence of such structures is the use of thermographic means to analyse temperature distributions on the wall bounding the flow. The idea is based on the, often-suggested, assumption that coherent structures are the hydrodynamic origin of coherent thermal structures on the heated wall (Iritani et al. 1983; Hetsroni and Rozenblit 1994; Hetsroni et al. 1997a, b). The knowledge of the convection velocity of these coherent structures can provide useful information on the various transport properties.

The convection velocity (propagation velocity of perturbations in the turbulent flow) has been measured by many methods. Favre et al. (1957) derived it for large eddies from space–time correlation measurements. Willmarth and Woolridge (1962) and Wills (1964, 1971) measured directly the convection velocity of the burst event. The database obtained from direct numerical simulation of a turbulent channel flow and the analyses of Kim and Hussain (1993) provides the detailed information on the propagation of velocity, vorticity and pressure perturbations in a turbulent shear flow. Bagheri and White (1993) made hot wire anemometry measurements over a heated flat plate. Space–time correlations of air temperature fluctuations were determined as a function of a dimensionless length in the direction normal to the wall. The convection velocity of the temperature fluctuations was found to be closely related to the convection velocity of the streamwise velocity fluctuations. The lowest height considered in this study for the evaluation of the convection velocity of temperature fluctuation structure was at $y^+ = 75$, and the Prandtl number was $\mathrm{Pr} = 0.7$.

For fluids characterized by relatively small thermal diffusivity (high Prandtl number), it is reasonable to assume that the convection velocities of temperature and velocity fluctuations are about the same throughout the boundary layer. If the temperature differences within the boundary layer are kept small, the buoyancy effects can be neglected. In such a case, the thermal pattern convected by the flow behaves in a similar way to an ink dye (passive scalar) used for flow visualization, reproducing its main features (Herman et al. 1998). The idea for the present study is based on the assumption that observations of these thermal patches at the wall may reflect characteristics of coherent structures of the flow. The quantitative visualization of the transient thermal fields can be easily made using widely spread infrared (IR) scanning thermography (De Luca et al. 1990; Carlomagno 1997).

The objective of the present study is to apply recent advances and improvements in the technique of PIV to the analysis of the behaviour of the temperature field observed on the channel wall. The image velocimetry technique initiated in the 1970s for full field velocity measurements as an optical correlation of Young's interference fringes (Backer and Fourney 1997) received an enormous boost with the development of digital image acquisition and analysis methods. Many PIV evaluation methods are based on correlation schemes, which are accelerated by the fast Fourier transform (FFT) (Adrian 1991; Willert and Gharib 1991). Tokumaru and Dimotakis (1995) developed another evaluation method reported as image correlation velocimetry. Particle tracking velocimetry was used to evaluate the 3-D temporal flow field (Mass et al. 1993). Gui and Merzkirch (1996) introduced a method of tracking ensembles of particles. Each of these methods has its specific advantages and drawbacks. Comparative studies of different PIV evaluation methods have been done recently by Fei et al. (1999) and Gui and Merzkirch (2000).

The aim of the present study is to determine whether the alternation of thermal streaks measured at the wall can be correlated with the main flow features. It is important to understand that, unlike the classical PIV technique, our method attempts to track thermal patterns appearing as large objects with unclear and variable boundaries. Similar images obtained in combustion studies were used to track thermal patterns in the gas phase (Komiyami et al. 1996). The gaseous imaging velocimetry (GIV) method was introduced to evaluate the displacement of gas particles tagged by laser-induced fluorescence (Grünefeld et al. 1998). It appeared that the traditional correlation technique might be successfully applied to evaluate such images. However, due to the limitations typical of the FFT-based PIV methods, the resulting displacement field is quite sparse, with a number of spurious vectors generated. Further improvement in tracking the motion of irregular flow features seems to come from computer vision. A good comparison of these methods can be found in Vérestoy et al. (1999). One such method, based on the improved optical flow (OF) algorithm (Quénot et al. 1998a), is applied in the present paper to track the displacement of the thermal patterns.

The present article describes our efforts to analyse sequences of IR images taken on the heated bottom of the flume. The analysis is verified in a well-defined test, where a thin heated wire is moved along the channel and the thermal image created by the wire on the foil is recorded. Our preliminary experiments indicate that the analysis of the thermal patterns created by the coherent structures of turbulent channel flow can become a useful tool for both qualitative and quantitative data collection on the boundary layer flow properties in a variety of channel flow problems.

2
Flow arrangement

The experimental setup for the investigation of temperature fields on the heated surface is shown in Fig. 1. It includes an open flume (Hetsroni and Rozenblit 1994), consisting of a rectangular stainless steel channel (4.3 m long, 0.32 m wide and 0.1 m deep), entrance and exit tanks and a pump forcing the circulation of constant temperature water. The flow depth is 0.037 m and the hydraulic diameter is 0.066 m. Care was taken to eliminate vibration, wave formation at the inlet and reflections from the outlet. A fully developed flow was established in the region beyond 2.5 m downstream from the inlet of the flume. The measurements of the water velocity profile and the distribution of the root-mean-square (r.m.s.) values of

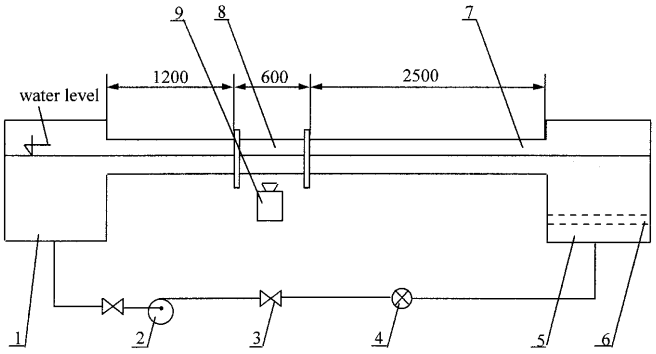

Fig. 1. A schematic diagram of the experimental facility: *1* outlet tank; *2* pump; *3* control valve; *4* flowmeter; *5* inlet tank; *6* grid; *7* open channel; *8* test section; *9* IR camera

streamwise velocity fluctuations confirmed this. The measurements were done at the centreline of the flume, i.e. at $z = 0$. Velocity measurements were done by means of a hot film anemometer. The standard 90° conical probe was connected to a traversing mechanism with a spatial resolution of 10 μm. The measured value of the average streamwise water velocity was $U = 0.25$ m/s. The experimental value of shear velocity $u^* = 0.0133$ m/s agrees well with the "logarithmic law of the wall": $U^+ = 2.5 \ln(y^+) + 5.0$.

The heated test section at the bottom of the flume was made of a constantan foil, 50 μm thick, which was located at a distance of 2.5 m from the channel entrance. The temperature distribution on the wall can be considered as a trace of the flow structure near the wall, i.e. the structures in the turbulent boundary layer are the ones that cause the temperature variation on the wall, including the thermal streaks.

Throughout this paper, x, y and z denote the streamwise, wall-normal and spanwise directions, and U, u, u_v and w, w_v denote mean flow velocity and convection velocities of thermal pattern, or velocity fluctuations, in the streamwise and spanwise direction, respectively. Velocity, length and time are normalized by wall units as $U^+ = U/u^* \equiv U/(\tau_w/\rho)^{0.5}$, $l^+ = lu^*/\nu$, $t^+ = tu^{*2}/\nu$, where τ_w, ρ and ν denote wall-shear stress, density and kinematic viscosity.

3
Data acquisition, apparatus and procedure

The image acquisition system consisted of an IR scanner, S-VHS video recorder, computer, display and 8-bit frame grabber.

The radiometer has a typical minimum detectable temperature difference of 0.1 °C, a time response of 25 frames/s and a horizontal resolution of 256 physical pixels/line. The radiometer was located at a distance of 0.5 m, and the IR image created on the foil was recorded from below. The foil was very thin (50 μm) and had negligible thermal inertia. It was shown (Hetsroni and Rozenblit 1994; Hetsroni et al. 1996) that the temperature difference between the two sides of the foil is about 0.1 °C and the frequency response of the system is about the same as the acquisition frequency of the IR camera. Therefore, we may assume that the thermal pattern observed by the camera corresponds to temperature fluctuations in a thermal boundary layer of the flow. The image had 256 intensity levels and was recorded on video tape of the S-VHS format as a conventional "interlaced" video scan pattern of 25 frames/s. The experiments were carried out at a constant heat flux from the heated foil.

The video was then used in playback mode to analyse the data. The video frames were captured, digitized using the DT-3155 frame grabber and stored as 768 × 576-pixel images with the 256 intensity levels. Each image sequence contained up to 50 frames. The digitized images were subsequently analysed by image processing software.

4
Image analysis

Once a set of picture data had been digitally captured and stored, the result was a succession of 50 sequentially recorded image frames depicting the temperature field on the foil at discrete instances in time. The incoming video signals representing IR images were transformed pixel by pixel into intensity maps. The digitized image has a size of 768 × 576 pixels, whereas the useful area representing thermal image covers 740 × 450 image pixels. Temperature was determined by relating the 256 gray levels to the temperature calibration function of the IR detector. Extracting image features found within the selected gray level bandwidth, regions of specified temperature were filtered out.

The spatial correlation method implemented in the analysis of the experimental data is one in which the temperature correlation coefficients are obtained on a point-by-point basis. This correlation coefficient is a measure of the similarity between the two temperature fluctuation signals. Instead of identifying discrete spots and tracking them from one image to the next, two-dimensional correlation between thermal patterns found within the analysed windows were used to determine the convective velocity of a thermal pattern. It allows for the identification of the trajectory of the thermal spots.

To evaluate the displacement of the thermal spots, initially the typical FFT-based PIV approach was used. In the implemented PIV technique (see Hiller et al. 1993), pairs of images to be correlated are obtained using a full video frame. Hence, the minimum time delay between images was $\Delta t = 40$ ms. By considering pairs of frames in a sequence taken at longer time steps, this time interval can be easily increased. Small sections of both images, called *interrogation windows*, are cross correlated and the average spatial displacement of the particles is evaluated. The mean displacement is provided by the position of the cross-correlation peak. The velocity in the interrogation window is obtained by dividing the displacement by the time interval Δt. The relative amplitude of the cross-correlation peaks with respect to the noise level is an indication of the measurement quality and is used as a criterion for the velocity vectors validation procedure.

Interrogation windows of 64 × 64 and 128 × 128 image pixels, 50% overlapped, were used to evaluate thermal spot displacement. The mean displacement is determined with a resolution of up to 1 pixel through interpolation, cor-

responding to about 0.24 mm for the physical size. The minimum velocity u_{min} which the system is able to resolve is given by the ratio between the minimum detectable displacement of thermal spots and the time interval Δt. For the pair of subsequent frames, we obtain $u_{min} = 6$ mm/s. This value can be considerably reduced by selecting pairs of images taken at a longer time interval Δt within the same sequence. In fact, for a sequence of 50 images, a theoretical limit for the velocity u_{min} becomes 0.12 mm/s. The maximum reliable displacement detectable by FFT-based PIV evaluation is limited by the dimensions of the interrogation window (Adrian 1991). In practice, it does not exceed 0.5 of the interrogation window size. For a 128×128-pixel window, it corresponds to a maximum resolvable velocity u_{max} of about 0.35 m/s.

The IR image created on the wall differs significantly from that created by seeding with particles used to evaluate the flow velocity by the PIV method. Instead of discrete dots, we observe large spots covering the image. The velocity vectors must be determined for each thermal spot displacement, representing its mean evolution in time. For two-dimensional cases, this could be directly correlated with the convective components of the flow velocity fluctuations. However, the coherent wall structures consist of high velocity regions and low-speed streaks very close to the wall. This configuration is periodically disturbed by ejections from the wall layer into the outer flow and sweeps back to the wall, generally referred to as "bursts". Kaftori et al. (1994) suggested that this pattern could be described as an expanding spiral, wound around a funnel that is laid sideways in the direction of the flow. These velocity fluctuations produce strong modulation of the temperature field in the wall layer. Hence, the size and intensity of the thermal spots observed at the wall varies in time. This effect is similar to the appearance and disappearance of particles crossing an illumination plane for classical PIV. It causes a broadening of the cross-correlation peak, reducing the overall evaluation accuracy. In our experiments, the third velocity component becomes noticeably large in regions where the funnel vortices separate from the wall. The "out of plane" bursts deteriorate the temperature pattern, which appears as false velocity vectors in the PIV results. The typical validation approach of classical PIV procedures substitute such vectors by averages among the surrounding ones. In our case, this approach is not acceptable. In fact, the temperature field in such places is discontinuous. Hence, we rather leave the raw results of the cross correlation as they are, limiting our analysis to the regions granting high correlation coefficients. The remaining regions of low correlation factor could eventually be interpreted as possible locations of turbulent bursts.

As already mentioned, images of large thermal spots radically differ from the images typical for PIV. This may seriously degrade the accuracy for the typical FFT-based evaluation procedure. Further improvement in the quality and smoothness of the evaluated fields was obtained applying a method recently developed by Quénot et al. (1998a). Using the OF algorithm, the method is free of the typical PIV limitations, still preserving high accuracy of the evaluated velocity field. The method is based on the search of a transformation that relates the second image to the first one by minimizing the distance between them. The matching is performed iteratively, starting from several parallel overlapping strips sliced from the both images. For every pair of strips, an optimal match is searched. The accuracy of the matching result is refined by reiterating the matching procedure several times in a pyramidal fashion with successively reduced spacing and width of the strips. It results in a subpixel accuracy of the displacement matching. Further improvement in the evaluation accuracy is possible if a longer image sequence is available. It is obtained by simultaneous matching of the generalized multi-pixel distance defined for the analysed image sequence. The continuous matching of the image texture used by the method, contrary to the classical PIV method, does not need quasi-periodic image structure produced by particle flow seeding. Hence, similarly to image correlation velocimetry, the method is well suited to analyse particleless images. In fact, the OF-PIV method was successfully used to analyse motion visualized by smoke or to evaluate growth of vapour bubbles (Quénot et al. 1998b). However, application of the OF-PIV costs immense computational time. A typical evaluation time for a 400-MHz CPU exceeds 3 h for a sequence of three images, compared with a few minutes using FFT-PIV for a pair of images. Therefore, use of OF-PIV for more profound statistical data analysis was not possible at the time when the work presented here was carried out.

5 Testing procedure

The ability of the FFT-based PIV method to determine correctly an average value of the convection velocity of the thermal pattern has been evaluated by comparison of experimental data with results obtained using a PIV routine.

It was very important to verify the method by some well-defined test, in which we know the velocity of thermal field propagation from both the calculations based on the new method and an additional independent source. This purpose was achieved using a special device, which moves a thin wire along the channel (in the x direction). The 25-μm wire was stretched in the spanwise direction (z direction) over the foil, so that a good thermal contact between the two was established. A DC current heated the wire, while the foil was initially at room temperature. Heat was conducted to the foil from the wire. The device makes it possible to move the wire with a constant velocity (Fig. 2). Thus, we know the exact wire location at any instant, and can match this location with the thermal image created by the wire on the foil. On this basis, the optimal bandwidth and window size were determined for different source velocities, as described below.

Figure 3 shows a typical image of a thermal field created on the foil by the moving hot wire. The size of the image was 170 mm in the x direction and 130 mm in the z direction. The image resolution was one physical pixel of IR sensor, i.e. 0.66 mm and 0.50 mm in the streamwise and spanwise directions respectively. Displacement of the thermal pattern at two different velocities of the linear source was examined, and 12 series of tests were conducted for each value of the linear source velocity. The

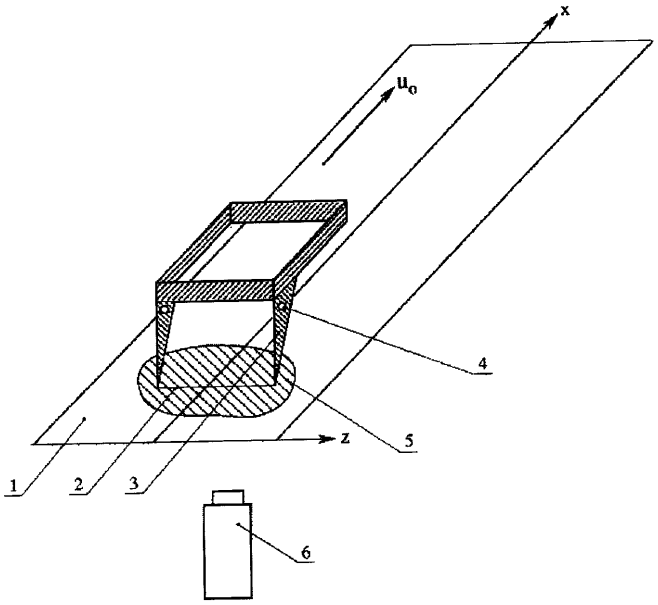

Fig. 2. A schematic of the setup with moving heated wire: *1* constantan foil; *2* linear heat source; *3* support; *4* electric contact; *5* thermal field on the foil; *6* IR camera

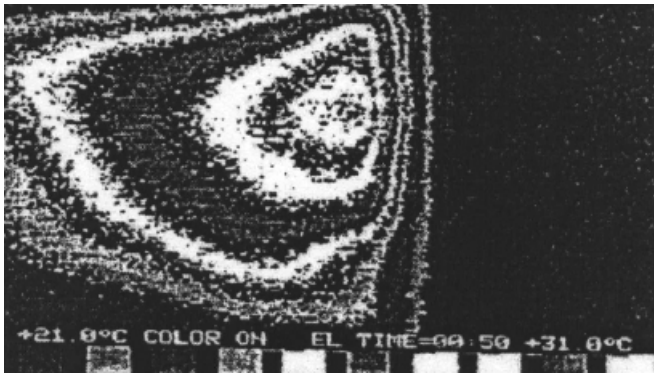

Fig. 3. IR image of a thermal pattern created on the foil by the moving heated wire. The thermal structure is emphasized using a false colour look-up table

displacement of the thermal pattern during experiments was recorded on the videotape, and the time of a given displacement was measured. The velocity values of the linear source were $u_o = 4.7 \pm 0.1$ mm/s and $u_o = 18.8 \pm 0.5$ mm/s.

For each value of u_o, 12 image files were analysed using the FFT-based PIV routine. The images were captured at different time separations between frames, and the effect of time interval on the evaluation error was studied. The error of evaluation is calculated as time and space averaged standard deviation. The selected bandwidth of gray level was 30; two sizes of the interrogation window, namely, 64×64 and 128×128 pixels, were utilized. The error of evaluation is shown in Fig. 4 for the heat source moving with velocity of 18.8 mm/s. We may note that the evaluation error increases with the size of interrogation window and is strongly related to the time interval between pairs of images. Such behaviour is typical for the

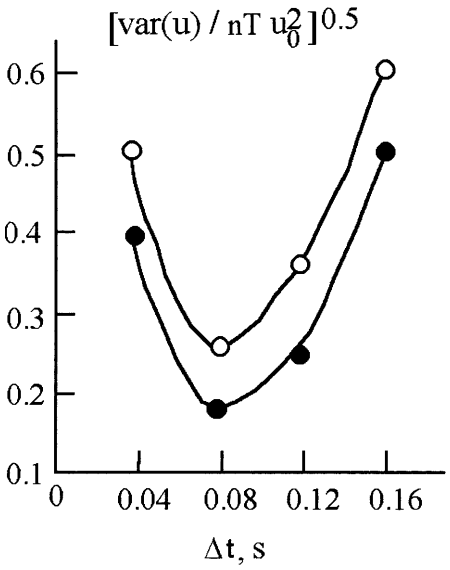

Fig. 4. Normalized mean error of PIV velocity evaluation for the heat source moving with velocity $u_o = 18.8$ mm/s; effect of the image interval time Δt: *closed circles*, interrogation window size 64×64 pixels; *open circles*, interrogation window size 128×128 pixels

PIV evaluation. Too large an interrogation window and too short a time interval deteriorate evaluation for low-speed, fine-flow structures, whereas the opposite configuration limits the maximum detectable displacement. It was found that, for the case investigated, optimal evaluation results (relative velocity error 13%) are obtained for a 64×64 interrogation window and a time interval between images of 80 ms.

The images of thermal spots display variation in the temperature as 256 gray levels. For the present image analysis, it seems reasonable to limit the bandwidth of the image, tracking selected characteristics, for example, the hot spots or cold spots only. To find the optimal gray level bandwidth, a sequence of images was evaluated varying it between 30 and 150. Figure 5 shows that, for the sequence investigated, the "best" bandwidth is in the range of 30–60. It appears that too large a bandwidth, covering regions of different temperatures, generates additional noise, degrading image correlation. It may indicate that hot and cold spots produced by the wire were not moving in phase. Decreasing bandwidth, we arbitrarily select only a certain range of temperature fluctuation for further analysis; this seems to improve the image correlation. Hence, the bandwidth of 60 gray levels was chosen as optimal for further experimentation.

We note here that the recorded image is in fact degraded, because of the limited spatial resolution of the IR imaging system. Both shape and size of the thermal spots varies strongly as they are conveyed across the interrogation window. Hence, the FFT-based PIV method exhibits a relatively large error of evaluated streamwise velocity (13%). Somewhat better result (8% error) could be obtained applying the OF-based PIV method of image evaluation. The method does not need any window adjustments and provides a smooth velocity field with the displacement vector calculated for each pixel of the

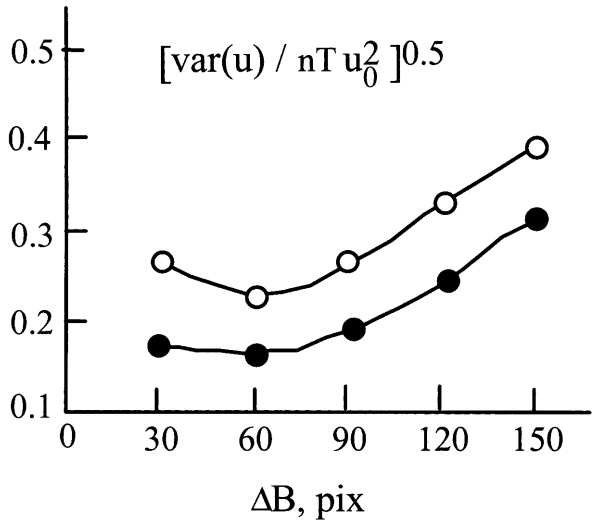

Fig. 5. Normalized mean error of PIV evaluation for the heat source moving with velocity $u_o = 18.8$ mm/s, $\Delta t = 0.08$ s; effect of gray level bandwidth: *closed circles*, interrogation window size 64×64 pixels; *open circles*, interrogation window size 128×128 pixels

image. In fact, for images with a fine texture, the spatial resolution of the method is limited by a camera resolution only. In our case, it is limited by IR sensor to about 0.6 mm.

To improve accuracy, several images of the sequence can be used simultaneously for displacement evaluation. In the present work, the best results were obtained using the OF-PIV method with three subsequent images taken at 40-ms intervals.

6
Measurements of thermal pattern convection velocity in the flume

In the following examples of measurements performed, we consider the flow of water at Re = 9,200 with the mean flow velocity $U = 0.25$ m/s. The heat flux from the heated foil is $q = 12$ kW/m^2, Prandtl number Pr = 7.1 and water temperature at the inlet is 20 ± 0.1 °C. The temperature variations in the range of 2 °C were observed at the wall section monitored using an IR radiometer.

A typical sequence of the formation and development of the temperature streak starts with the rise of small moving high or low temperature spots. These spots change their position and streamwise length. Figure 6 shows a pair of IR images of the wall temperature taken at a time interval of 40 ms. The high and low temperature streaks, clearly seen on the wall surface, indicate the presence of the coherent structures advected by the main flow. The bright patches correspond to regions of higher temperature on the bottom of the flume. The streamwise flow structures persist for some time until strong mixing (vertical burst) leads to their disappearance. The cold regions (dark streaks) indicate locations of the strong vertical motion (wall ejections and in-sweeps), which is responsible for the increased heat transfer. They appear to move faster and often overtake adjacent bright streaks. The high and low temperature streaks may interact with each other too. The present examination was concentrated on the downward moving spots of high temperature (bright range of gray levels), as they were thought to be associated with low-speed flow structures.

The evaluation procedure applied consists of the following steps performed for each sequence of images:

- Acquisition of a long sequence of images using an IR sensor and video recorder
- Digitalization of IR images using a DT3155 frame grabber (due to the limited computer memory only up to 50 images could be taken for one sequence)
- Selection of the appropriate section of the image
- Selection of the gray level band and time interval for image correlation
- Image correlation for the sequence
- Analysis of the velocity vector fields: velocity extreme, mean value, histogram of streamwise velocity
- Selection of the velocity band representing convective motion of the hot spots, evaluation of the spatial and temporal average for hot spots convective motion
- Evaluation of the temporal velocity fluctuations at the arbitrary selected points for the sequence

An example of an evaluated propagation velocity for the sequence displayed in Fig. 6 is shown in Fig. 7. The vector field was evaluated for the gray level band of 175–255 using the OF-PIV procedure. We may note that the convection

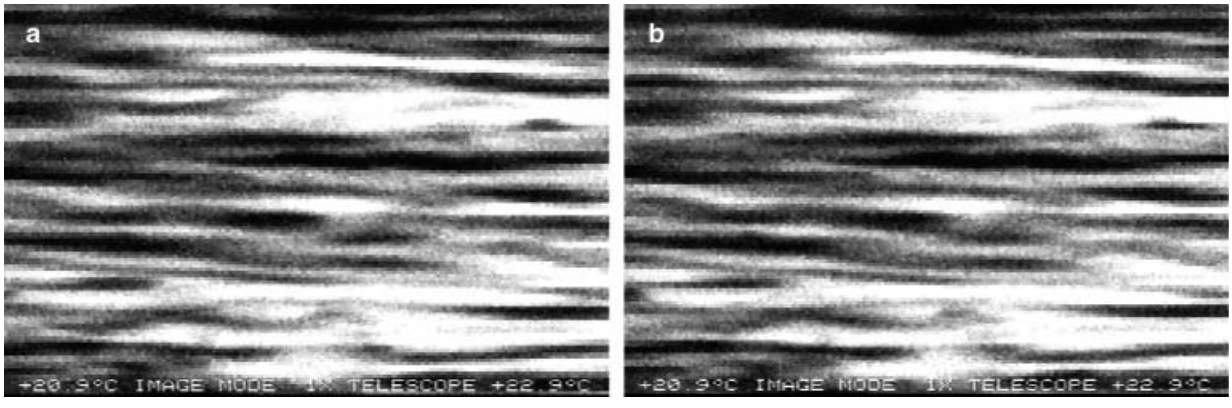

Fig. 6. Instantaneous temperature distribution observed by IR sensor on the bottom of the flume in a turbulent flow. Two images taken at a time interval of 40 ms. Thermal pattern of the images covers an area 170 mm (width) × 130 mm (length) of the foil

motion varies in the direction as in the magnitude, but a strong streamwise velocity bias transporting thermal spots from left to right is clearly visible. The contour plots in Fig. 8 show maps of two components of the velocity vector field. It can be seen in Fig. 8a that the streamwise velocity preserves the main features of the temperature strips. The propagation velocity varies from peak values close to $10u^*$ to slightly negative values, where direction reversal of the spots' motion was observed. Figure 8b shows the spanwise component of the hot spots' velocity. Their mean velocity was close to zero and both negative, and positive deflections of the motion form a chessboard pattern in the contour plot.

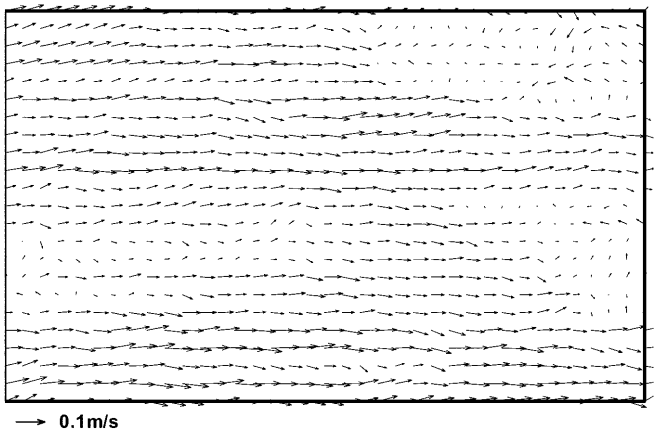

Fig. 7. Instantaneous velocity vector field of thermal spots evaluated from IR images shown in Fig. 6; OF-PIV method, selected for evaluation gray level bandwidth of 175–255; displayed area of 740 × 450 pixels corresponds to 170 mm × 118 mm section of the foil

Figure 9 shows an example of the transient behaviour of the pattern. At the arbitrary selected point, both the components of the streak velocity are extracted from the evaluated vector fields and plotted for a period of 1.2 s. The displayed plots demonstrate well a striking feature of the temperature field on the heated wall in a turbulent flow, i.e. that coherent thermal structures (CTS) behave like pulses in time. It is significant that not only the z component but also the x component of the convection velocity shows these eruptive events. The time variation of convection velocities, shown in Fig. 9, indicates that the convection velocity in the x direction is much higher than that in the z direction; thus, the observed structures are nearly aligned in the streamwise direction. Although the streamwise propagation velocity varies, its time average has a non-zero positive value. It clearly indicates that the thermal pattern propagates in the streamwise direction. This motion is associated with the propagation velocity of the velocity fluctuations in the turbulent flow.

The transverse component of the convection velocity w varies with time, with nearly symmetrical positive and negative amplitudes, when analysed for a longer time interval. In fact, the time and space averaged spanwise velocity of the sequence is close to zero.

The streamwise velocity fluctuations are related to the geometry of the streak pattern. The low- and high-speed streaks passing the selected point of observation contrib-

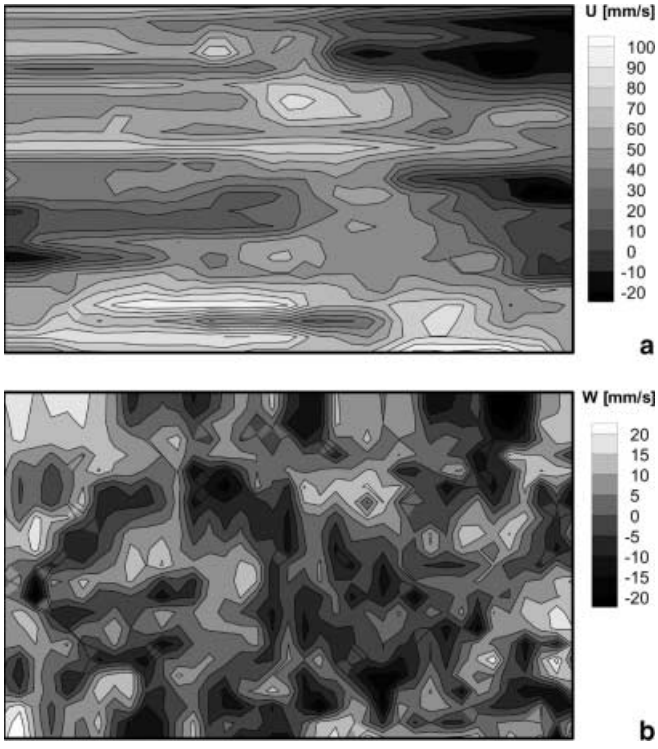

Fig. 8a, b. Velocity contour plots evaluated form the vector field shown in Fig. 7: **a** streamwise velocity component; **b** spanwise velocity component

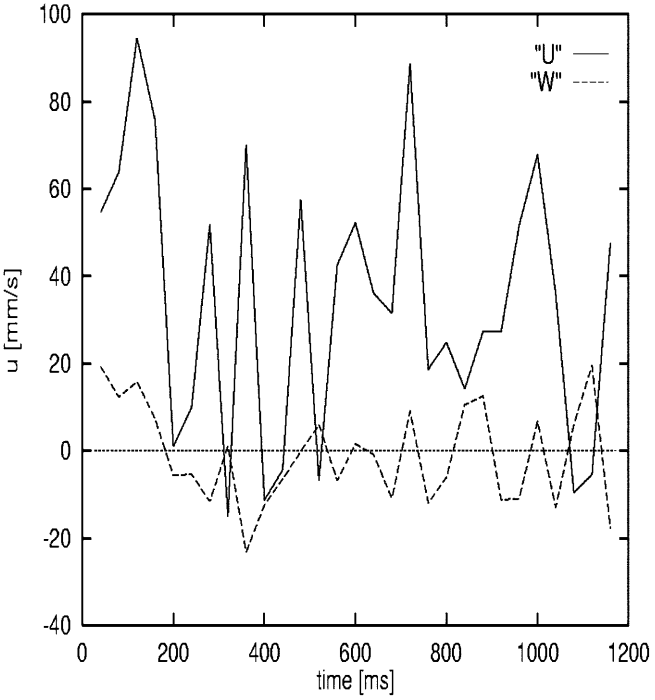

Fig. 9. Time variation of convection velocity of coherent thermal structures on the heated wall extracted for an arbitrary point of the evaluated velocity vector field: *solid line*, streamwise component; *dashed line*, spanwise component

ute to the transient pattern. For a sufficiently long observation time, their main characteristics will become space independent. Then, analysis of the full field temporal behaviour of both velocity components may deliver a large amount of data for statistical analysis of the flow. But even our relatively short sequence may be used to evaluate the characteristic velocity of the observed thermal structures. For this purpose, we need to identify them in the velocity vector field. Looking at the velocity contour plots shown in Fig. 8a, we may note bright patches where a high displacement velocity was found. We assume that they indicate the location of moving thermal spots. To evaluate their characteristic velocity, some discrimination technique must be applied. We arbitrarily assume that the centroid of pixels with a streamwise velocity above 85% of maximum velocity of the analysed field represents displacement of the hot spots. By taking the time and space average of such discriminated velocity values, the mean streamwise velocity component of the hot spots was calculated for the whole sequence. This value for the analysed sequence of 31 images was 0.127 m/s, i.e. $9.54u^*$. By taking into account all streamwise velocity vectors, the time and space average obtained for the sequence was 0.048 m/s.

Assuming that coherent structures play a dominant role in transport phenomena in turbulent flows, it is interesting to interpret the turbulent transport of heat or mass in terms of the dynamics and transport properties of advecting coherent structures. In order to clarify the role of large-scale coherent structures in the heat transfer mechanism, we compare our results with the propagation velocity of fluctuations in a turbulent channel flow of water reported by Kim and Hussain (1993). As shown in that study, the propagation velocity for velocity fluctuations is $u_v^+ = 10$ for $0.2 < y^+ \leq 10$. The upper limit of the mean velocity of the temperature fluctuations on the heated wall obtained in the present study is $u_v^+ = 9.54$. Hence, under the conditions of the present experiment, the time and space averaged dimensionless value of CTS propagation velocity is close to 10, indicating strong correlation between the measured propagation of the hot spots and the typical convective velocity of the turbulent velocity fluctuations. This is in agreement with the propagation velocity of the large-scale temperature fluctuation structures obtained by Bagheri and White (1993).

7 Conclusions

These results of the analysis demonstrate the ability of the tracking algorithm to calculate the trajectory vectors with widely varying velocity magnitudes in the given temperature field. The stochastic character of the turbulent motion is reflected in the fluctuating thermal pattern observed at the selected section of the channel wall. These structures are believed to be responsible for the turbulent heat transport and therefore are very important in determining the scalar transport properties of turbulence. The temporal and spatial analysis of long time sequences of thermal images may allow us to evaluated the basic characteristics of the underlying fluid flow. It has already been demonstrated that the mean convective velocity of coherent structures can be relatively well evaluated from the thermal pattern dynamics. It is worth noting that the method allows us to obtain this velocity without any optical or mechanical access to the flow. This, combined with the known bulk flow velocity in the channel, permits a description of the main properties of the analysed flow. We believe that other scalar characteristics, such as bursting period, mean turbulent energy and diffusion constants, can be correlated with the observation of the transient behaviour of the thermal pattern.

However, it must be considered that our observations are limited to two-dimensional projections of the flow structure, and its quantitative interpretation needs additional information about the main flow. These experiments have only demonstrated the qualitative behaviour of the thermal streaks. Full field measurements of the main flow characteristics performed for various flow conditions combined with monitoring of the thermal streak dynamics may provide a sufficient amount of data to build and verify models relating the turbulent flow characteristics with their scalar "finger prints" at the wall.

References

Adrian RJ (1991) Particle imaging techniques for experimental fluid mechanics. Annu Rev Fluid Mech 23: 261–304

Backer DB; Fourney ME (1997) Measuring fluid velocities with speckle patterns. Opt Lett 1: 135–137

Bagheri N; White BR (1993) Experimental measurements of large-scale temperature fluctuation structures in a heated incompressible turbulent boundary layer. Int J Heat Mass Transfer 36: 907–918

Carlomagno GM (1997) Infrared thermography and convective heat transfer. In: Giot M, Mayinger F, Celata GP (eds) Experimental heat transfer, fluid mechanics and thermodynamics. Edizioni ETS, Pisa, pp 29–43

De Luca L; Carlomagno GM; Buresti G (1990) Boundary layer diagnostics by means of an infrared scanning radiometer. Exp Fluids 9: 121–128

Favre A; Gaviglio J; Dumas R (1957) Space–time double correlations and spectra in a turbulent boundary layer. J Fluid Mech 2: 313–342

Fei R; Gui L; Merzkirch W (1999) Comparative study of correlation-based PIV evaluation methods. Mach Graphics Vision 8: 571–578

Grünefeld G; Finke H; Bartelheimer J; Krüger S (1998) Gaseous imaging velocimetry: ein neues 2D-Verfahren der Strömungs- und Verbrennungsdiagnostik. In: Tagungsband der 6. Fachtagung "Lasermethoden in der Strömungsmeßtechnik", 28–30 September, Essen

Gui LC; Merzkirch W (1996) A method of tracking ensembles of particle images. Exp Fluids 21: 465–468

Gui LC; Merzkirch W (2000) A comparative study of the MQD method and several correlation-based evaluation algorithms. Exp Fluids 28: 36–44

Herman C; Kang E; Wetzel M (1998) Expanding the application of holographic interferometry to the quantitative visualization of oscillatory thermofluid process using temperature as tracer. Exp Fluids 24: 431–446

Hetsroni G; Rozenblit R (1994) Heat transfer to a liquid solid mixture in a flume. Int J Multiphase Flow 20: 671–689

Hetsroni G; Rozenblit R; Yarin LP (1996) A hot-foil infrared technique for studying the temperature field of a wall. Meas Sci Technol 7: 1418–1427

Hetsroni G; Zakin JL; Mosyak A (1997a) Low speed streaks in drag-reduced turbulent flow. Phys Fluids 9: 2397–2404

Hetsroni G; Mosyak A; Rozenblit R; Yarin LP; Ziskind G (1997b) Experimental investigation of temperature fields on smooth

and rough walls in a turbulent boundary layer. In: Giot M, Mayinger F, Celata GP (eds) Experimental heat transfer, fluid mechanics and thermodynamics. Edizioni ETS, Pisa, pp 1841–1853

Hiller W; Koch St; Kowalewski TA; Stella F (1993) Onset of natural convection in a cube. Int J Heat Mass Transfer 36: 3251–3263

Iritani Y; Kasagi N; Hirata N (1983) Heat transfer mechanism and associated turbulence structure in the near wall region of a turbulent boundary layer. In: Fourth Symposium on Turbulent Shear Flows, Karlsruhe, Germany, 12–14 September, pp 17.31–17.36

Kaftori D; Hetsroni G; Banerjee S (1994) Funnel-shaped vortical structures in wall turbulence. Phys Fluids 6: 3035–3050

Kim J; Hussain F (1993) Propagation velocity of perturbations in turbulent channel flow. Phys Fluids 5: 695–706

Kim J; Moin P (1989) Transport of passive scalars in a turbulent channel flow. In: Turbulent shear flows, vol 6. Springer, Heidelberg Berlin New York, pp 85–96

Komiyami M; Miyafuji A; Toshimi T (1996) Flamelet behaviour in a turbulent diffusion flame measured by Rayleigh scattering image velocimetry. In: The 26th Symposium (International) on Combustion, pp 339–346

Mass HG; Grün A; Papantoniu D (1993) Particle tracking velocimetry in three-dimensional flows. Part I. Photogrammetric determination of particle coordinates. Exp Fluids 15: 133–146

Quénot GM; Pakleza J; Kowalewski TA (1998a) Particle image velocimetry with optical flow. Exp Fluids 25: 177–189

Quénot GM; Pakleza J; Kowalewski TA (1998b) Particle image velocimetry using optical flow for image analysis. In: The 8th International Symposium on Flow Visualisation, Sorrento, Italy, 1–4 September, CD-ROM Proceedings (ISBN 09533991-09). G.M. Carlomagno and I. Grant, Edinburgh, pp 47.1–47.11

Robinson SK (1991) Coherent motions in the turbulent boundary layer. Annu Rev Fluid Mech 23: 601–639

Robinson SK (1993) The kinematics of turbulent boundary layer structure. NASA TM-103859, pp 490–501

Tokumaru PT; Dimotakis PE (1995) Image correlation velocimetry. Exp Fluids 19: 1–15

Verestóy J; Chetverikov D; Nagy M (1999) Digital image velocimetry: a challenge for feature based tracking, Mach Graphics Vision 8: 553–570

Willert CE; Gharib M (1991) Digital particle image velocimetry. Exp Fluids 10: 181–193

Willmarth WW; Woolridge CE (1962) Measurements of the fluctuating pressure at the wall beneath a thick turbulent boundary layer. J Fluid Mech 14: 187–210

Wills JAB (1964) On convection velocities in turbulent shear flows. J Fluid Mech 20: 417–432

Wills JAB (1971) Measurements of wave-number phase velocity spectrum of wall pressure beneath a turbulent boundary layer. J Fluid Mech 45: 65–90